University of Waterloo
Department of Systems Engineering

Final Report:
Modelling Neuronal Impact Following a Brain Injury

Alexis Bader (20942115) | Livia Murray (20928120) | Mackenzie Snyder (20932690) |
Navalan Thadchanamoorthy (20933153) | Adele Younis (20944650)

BME 355: Final Project
April 8th, 2024

Abstract

Understanding the neurophysiological mechanisms underlying concussions is crucial for injury prevention, diagnosis, and treatment. In this study, a computational model to investigate the impact of concussions on neuronal function was developed, focusing on the disruption of sodium channels in the brain. The model integrates the Head Injury Criterion (HIC) to quantify concussion severity and modifies the Hodgkin-Huxley neuron model to simulate the effects of axonal trauma. Additionally, synaptic transmission was modeled to interpret the communication between neurons. The results demonstrate that concussion severity, controlled by factors such as impact velocity and the percentage of damaged ion channels in neurons, directly affects neuronal activity. Higher impact velocities lead to decreased sodium channel activation and slower action potential transmission, while the percentage of active sodium channels plays a significant role in determining the magnitude and regularity of action potential spikes. Optimization techniques further elucidate the relative importance of these factors in predicting injury severity. Although the model simplifies certain aspects of neuronal behavior, it provides valuable insights into the physiological consequences of concussions. Future research efforts should focus on incorporating experimental data and refining the model to enhance its predictive accuracy and clinical utility. Overall, the computational approach offers a promising framework for understanding and addressing the complexities of concussions, with potential applications in injury prevention and personalized healthcare, and collision safety.

Introduction

Concussions are a prevalent form of traumatic brain injury (TBI), affecting millions of individuals annually and posing significant health risks [1][2]. A concussion refers to any neurological impairment stemming from forces applied to the head [3]. Signs of a concussion encompass, but are not restricted to, loss of consciousness, confusion, dizziness, headache, and visual disturbances [3]. As these symptoms typically dissipate over time, a concussion is characterized as a temporary disruption in neuronal function rather than irreversible cell death, influencing neurotransmission rates [3].

Primarily of interest in our investigation into concussion impact is the damage occurring to the sodium channels of neuron membranes in the brain after impact, and the resulting fluctuations in timings and magnitude of action potentials conducted during neurological activity. In order to quantify the relationship between the initial velocity of the head during an impact, and the neurological damage sustained, a modified Head Injury Criterion (HIC) was implemented to classify the likeness of mild, moderate and severe concussion [4]. This scale is commonly used to determine the likeliness of TBIs in crash dummies during automotive crash testing, and is employed generally here to correspond to a level of injury modeling on the neuron, via curve derivation and fitting. Damage is modeled using a voltage left-shift algorithm, which is translated throughout the Hodgkin-Huxley neuron groups and respective state variables. Through manipulating the severity of the concussion being simulated, a slower transmission speed across neurons in cases where force and the level of damage modeled was greater is expected. This change in transmission speed can be related to cognitive deficits seen during concussion, due to the limiting capacity of the brain for generation and remyelination [5], which may lead to cognitive impairment such as difficulties with memory, attention, processing, as well as motor impairments. The objective is to input an initial velocity at the time of impact, and receive action potential metrics from neurons resulting from the various levels of simulated damage.

In relevant prior works, computational neuroscience has developed models of the neuron as electrical circuits, with one of the most well used neuron models is the Hodgkin-Huxley (HH) model,

initially adapted from the LIF model. This mathematical model focuses on the behaviour of the voltage gated potassium and sodium ion-channels present within an axon [6]. An input into this model is the membrane capacitance, which responds to damage by degradation of sodium ion channels as represented in research done by V. Volman and L. J. Ng [7]. This causes additional leakiness in the sodium current model from HH, resulting in a new membrane current model [7].

Two different avenues for realism were explored; one focusing on the input voltage shift curve using HIC metrics and velocity values during crash test cases, and another expanding the neuron model for biological purposes to have multiple propagating spikes on a single neuron and synaptic transmissions to build a neuron network. The former was deemed more relevant to the concussion assessment problem space, and so the single spike neuron case is the focus of the following report. In the later model, the membrane current is what causes an action potential to propagate along the axon towards the synapses so the effects of axonal injury can be scaled up when studying synaptic transmission and full brain neuronal communication. Synaptic transmission has been demonstrated as a function of conductivity and current that passes through the synaptic cleft, as previously modeled by Gerstner et. al [8].

The simulated state-space model can be used to understand current concussion prevention instruments and their limitations. The model, with some adjustments for scaling, leads to a better understanding of the underlying damage on a smaller, while more abstract, scale of concussions at the single neuron. An understanding of concussion biomechanics as a neurological dysfunction resulting from force experienced on impact [3], is critical to several practices in injury prevention and medical diagnosis or treatment, rule changes in sports and return to activity, as well as general education and awareness. Primarily, we consider this model to be useful in the understanding of concussion prevention, and designing gear or safety equipment to prevent more severe TBIs, with an understanding of acceleration dynamics and how impacts at very magnitudes affect damage ratings, and thus cognitive impairment.

Methods

This model was implemented in three consecutive parts, with additional steps to optimize, validate, and verify the outcomes throughout. The first part of the model aimed to build a relationship between the severity of an injury and the damage it caused to the voltage-gated sodium (NaV) ion channels within an axon, based on the degree of impact. The second portion of the model adapted the Hodgkin-Huxley neuron model to accommodate for the different severity levels of axonal trauma. The final part of the model connects multiple neurons together through synaptic transmission. It is important to note, that the final part of the model was designed to solely model maximal axonal trauma, and was not integrated with the simulation trials discussed below.

I. Head Injury Criterion and Trauma Within Sodium Voltage-Gated Ion Channels

To model the degree of impact following trauma to the brain, the Head Injury Criterion (HIC) was used. The HIC is designed to quantify the cumulative effect of head acceleration over time during an automotive crash event. As a result, HIC is commonly used in the medical and automotive engineering industry to standardize the assessment for potential head injury in a patient or crash test dummy. The HIC equation, seen in **Appendix B, Equation 1,** works by integrating the head acceleration-time curve during impact, $a(T)$, over a specific duration time, t_2-t_1 [9]. This duration represents the time interval of the impact, corresponding to the greatest peak in the head-acceleration. Through literature, it is observed that deceleration graphs during crash testing are curve-fit to the summation of two bell-like curves occurring at different times, as seen in **Appendix B, Equation 2** [9]. Each bell-curve in these model's attributes to

one peak acceleration. Additionally, the deceleration curve of the crash assumes the head of the subject to always start and end stationary, spanning an average crash duration of 160 ms total [9]. To maintain consistency within the final model and model the worst case scenario, the duration, *d*, was kept constant at a value of 36 ms, the maximum acceptable duration of the HIC formula. Since the HIC equation only integrates for the duration about the greatest peak, the acceleration equation was modified in the final model to solely incorporate the greater of the peaks, as seen in **Appendix B, Equation 3**. This acceleration equation represents a simpler acceleration curve that divides the velocity, *v(t),* over the elapsed duration, in which the maximum change in velocity is observed at 93 ms. To produce a range of HIC values that could later be related to the traumatized neuron model, the HIC model was run with altering velocities.

The HIC associated with a 90% likelihood of the most severe concussion served as the benchmark for determining the conditions necessary to elicit the corresponding level of brain injury. Hence, an HIC value between 1000-1500 was attributed to causing a mild concussion, with HIC values of 1500 and 2000 set as the threshold values for moderate and severe concussions, respectively. HIC values below 1000 represent a healthy brain, devoid of any concussion indications. The nonexistent, mild, moderate, and severe concussion ranges of HIC values are attributed to velocity values of 10 m/s, 12 m/s, 14 m/s, and 18 m/s respectively. **Figure 2, in Appendix B**, represents the interpretation of HIC in relation to different severities of head injury, with the maximum abbreviated injury scale (MAIS) ranging from 0-6, corresponding from least to most severe brain injury [4]. For the purpose of this investigation, we will focus on MAIS levels 0 through 3, which correspond to no trauma, mild concussion, moderate concussion, and severe concussion, respectively.

II. Hodgkin - Huxley Model with NaV Ion Channel Trauma

The derivation of the modified Hodgkin-Huxley (HH) model is best understood through an electrical circuit representation, detailed in **Appendix A, Figure. 1**. This electrical circuit is composed of 3 separate branches, in parallel with an independent current source. Each branch within the circuit simulates different axonal membrane currents – one for the potassium voltage-gated ion channels, one for the sodium voltage-gated ion channels, and a third to encompass any additional leaky current [6]. To simulate the physiology of an axon, the capacitor, C_m, in this circuit functions as the axon membrane, facilitating the ingress and egress of ions within the axon [6]. The currents for both ion channels are determined from the activation and inactivation transition rates of the voltage-gated channels – *n, m,* and *h*. These 3 transition rates, alongside the voltage across the axonal membrane, V_m, represent the state variables in the original HH model [6]. The potassium ion channels are activated using the *n* transition variable, while the sodium ion channels are activated by *m*, and inactivated by *h*. Equations modelling these transition rates within neurons void of trauma can be seen in **Appendix B, Equations 8 - 16.**

As this study aims to simulate the physiological repercussions of concussions on the NaV channels, supplementary trauma parameters - fT, V_A, and V_L - have been incorporated into the NaV channel model. The initial parameter, fT, determines the percentage of NaV channels inhibited by trauma [7]. Furthermore, V_A and V_L mirror the coupled left shift (CLS) in the activation and inactivation of sodium channels within the traumatized axon [7]. Generally, the activation voltage, V_A, and inactivation voltage, V_L, of the NaV channels are equal post-trauma, allowing us to encompass voltage shift with one parameter, V_S [7]. The governing equations of the HH model can be found in **Appendix B, Equations 5-16, and 23**, and have been adjusted to incorporate the physiological effects of trauma on NaV ion channels, through fT and V_S. These specific adjustments are evident in **Appendix A, Equations 4, 17-22**

and 24, as they integrate forward and backward transition rate constants, *mT* and *hT*, for both sodium concentration states. It is crucial to acknowledge that as this model represents forces based on trauma impacts solely on the sodium channel, the potassium ion channel activation, *n*, was not altered. Constants used within these equations were retrieved through literature, and are seen in **Appendix C, Table 1** [7].

To define the physiological contrast between the three defined levels of concussion severity, it is assumed that the diagnosis of each concussion level is proportional to the damage caused within a single neuron. Suitable ranges for *fT* and V_S values were determined based on literature, which emphasized that *fT* should be within 0.1 to 1 and V_S should be between 10 – 20 mV [7]. A resultant CLS in the voltage activation under 10 mV does not appear to cause significant physiological symptoms of a concussion, with mild concussion symptoms beginning above this threshold [10]. A CLS of 14 mV is noted to map to symptoms of moderate concussion symptoms, and a 20 mV shift represents a high level of induced trauma for severe concussions [10]. To emphasize how the HIC model is integrated with the CLS, the input velocity maps to a HIC value within one of the four MAIS ranges. Both the velocity and fT parameters within this model are kept as individual inputs, to assess how changes in either input may impact the transmission of an action potential across an axon.

III. Synaptic Transmission

Synaptic transmission acts as the communication between neurons, and transference of action potentials along pathways to relay information. In order to expand the single neuron model, a group of an additional three neurons was added in simulation, and connected via current based synaptic transmission equations, as seen in **Appendix B, Equations 25-26**. The mathematical model of the current passing through the synaptic cleft, I_{syn}, depends on the difference between the membrane potential, V_m, and synaptic reversal potential, E_{syn}, alongside the conductivity of the neurotransmitter activated ion channels, g_{syn}, as seen in **Appendix B, Equation 25**. The synaptic reversal potential uses exclusively excitatory synapses, in which the corresponding value is 0 mV [8]. Additionally, **Equation 26 (see Appendix B)** models the time-dependent conductivity of the synaptic ion channels, g_{syn}, using an exponential decay focusing on the arrival time of a presynaptic action potential, t^f [8]. This combination of a heaviside step up, and exponential decay of current forms the bridge between the previously modeled neuron and the trailing one. Maximum voltages in damaged and healthy neurons were computed and input separately into the functions. The majority of the parameters chosen for this model are supported by literature, however, there are several constraints in the simulation accuracy when compared with the actual synaptic transmission of a neuron. To compensate for the simplifications made, certain parameters such as the synapse conduction, *gs_bar*, and the exponential decay rate, *tau*, were experimentally determined through a sensitivity analysis to ensure that the resultant spike meets the threshold for the action potential to occur. This includes scaling of the gain of the synaptic transmission to sustain a spike in the next neuron by the HH model, which is controlled primarily by the *gs_bar* variable. The onset of the synaptic transmission time is biologically accurate, to properly convey the relationship of the process in our time-dependent model for information transfer time, at a value of 0.5 ms [11]. The model was then further expanded by adding additional spikes to each 'neuron' model, to depict 4 neurons with 8 nodes of Ranvier each, to show a more biologically relevant model and simulation time across a group of neurons in network.

IV. Optimization

To optimize the initial conditions for the forward and backward transition rate variables, their equilibrium points were calculated using **Equation 27, as seen in Appendix B.** This equation calculates a

stability point, P, for each separate transition rate - *n, m, h, mT*, and *hT*, based on the relationships of their corresponding ion channels backwards and forwards transition rates. Within the HH model, this point can also be referred to as the open probability of ion channels [12]. For activation gates, a depolarizing shift in membrane potential increases P because the voltage dependency of α and β causes them to increase. Conversely, for inactivation gates, the change in α and β due to depolarization decreases P [12]. The original HH model assumes that α and β change instantly with voltage changes, but this does not lead to an instantaneous change in P. The rate at which P achieves its new value after a voltage change is determined is through the calculated difference between the rate of opening and the rate of shutting of the ion channel, as seen in **Appendix B, Equation 27**. Since the initial conditions within separate trials have altering parameter values for V_S and fT, the stability point was recalculated each simulation run to respond optimally to the state of the system.

Furthermore, to assess the relative significance of both V_S and fT, specifically aiming to determine which has a more significant impact on action potential transmission, a gradient descent optimization approach was employed. An objective function was built using a linear combination of the severe concussion results of V_{mT}, with a constant β_0, V_S as β_1, and fT as β_2 as seen in **Appendix B, Equation 28.** The values of fT and V_S were normalized in order to ensure uniform scaling, and the gradient descent algorithm was initialized with regression coefficients set to zero. Hyperparameters including the learning rate, defined as 0.0001, and the and the number of iterations, defined as 700, provided the optimal conditions for convergence which was determined experimentally. During each iteration, predictions were computed using the current regression coefficients and the mean squared error (MSE) was calculated as the discrepancy between predicted and actual values using **Appendix B, Equation 29**. Gradients of the MSE with respect to each coefficient were computed to update their values using **Appendix B, Equation 30-32**, iteratively moving towards minimizing error. Convergence of the algorithm was monitored by tracking the MSE across iterations, and the final values of the regression coefficients were obtained.

V. Verification and Validation

Steps were taken to verify and validate the accuracy and neurophysiological plausibility of the proposed model. To commence, each of the constants used within the HH model were obtained from experimental data found in literature, and can be seen in **Table 1, Appendix C** [6, 8]**.** This validates accuracy in the underlying structure of the model, cross-referencing the independent voltage sources and conductance values of each component seen in the electrical circuit diagram for the HH model, as seen in **Appendix A, Figure 2.** Similarly, within the synaptic transmission phase of the model, the experimentally derived values can be considered a form of validation, as those parameters were scaled from the plausible ranges shown in literature to establish the authenticity of the simulation. Additionally, as much of the inspiration for the axonal trauma model was taken from the work done previously by Volman and Ng, results obtained from our model were compared to theirs for validation purposes [7].

Furthermore, unit tests for both the HIC and HH models were written and executed to test various behaviours and parameters of the live model. In terms of the HIC model, two unit tests were written. The first test verifies that the maximum voltage shift value during each simulation trial is mapped to the HIC, corresponds to one of the threshold voltages of 0, 10, 14, and 20 mV. A second HIC unit test verifies the expected behaviour of the acceleration graph that the HIC equation integrates over. In particular, the second test verifies that the maximum peak in acceleration occurs at time equal to 93 ms, as this value was observed in literature discussing peak head-acceleration times during automotive crashes [9].

Similar to the HIC model, unit tests were also performed for the HH model. The first test within the file validates the input parameter *fT*, and verifies that it can only be set with values between 0.1 and 1, as this parameter represents the total percentage of traumatized NaV channels. Another test was implemented to test that the different values of voltage shift correspond to varying values of the membrane voltage with trauma, V_{mT}, with no impact on V_m. From there, two tests were written to test the equilibrium point, *P,* for the transition rates in both the healthy axonal membrane trace, and traumatized one. Within both these tests, the measured values for the ion channel transition rates are compared to their expected values obtained from literature. Finally, unit testing for the synaptic transmission verifies the behaviour of the functions for positive and negative input parameters, along with zero inputs. Additionally, the edge cases were analyzed for the functions that include spikes to ensure that the expected threshold is met.

VI. Simulation Trials

In order to run the model and assess the degree of axonal trauma based on concussion velocity, 9 simulation trials were run. A trial was run for each combination of *fT* percentage level with each MAIS level 2, 3, and 4 - corresponding to Vs values of 10 mV, 14 mV, and 20 mV. These simulations aid in the examination of both effects of axonal trauma on the NaV ion channels, being the CLS and percentage of traumatized NaV channels, on the axonal membrane voltage.

Results

From the implemented concussion model on neurons, many results can be drawn from viewing the changing state variables, plotting our Voltage vs Time curves, comparing our results with those in literature, and viewing the final graph of a single neuron action potential. With the objective of the model being to compare the neural axonal pathways in an ideal condition, to those with traumatized NaV ion channels following an mTBI, the results make it evident that our simulations succeeded.

The results from the acceleration over impact duration show a maximum spike in acceleration at 93 ms, which corresponds to the time when the maximum HIC value occurs. The acceleration and HIC curves have varying maximum points depending on the input velocity as seen in **Appendix A, Figure 3-6.** In order to view how the variations in percentage for fully functional NaV channels, *fT,* affected the state trajectories, the state variables were plotted in **Appendix A, Figure 7-9**. The plots demonstrate the change for the 10 mV shift, corresponding to a mild concussion for 10%, 50%, and 90% of the gates affected respectively. In particular, the mT and hT variables were altered based on the *fT* input level*,* while the n, m, and h variables remained constant throughout all simulations encompassing changing input values. This was expected as n, m, and h are the state variables corresponding to a healthy neural action potential. The results measured for the state variables n, m, and h were validated using results in literature, as the two sets of values aligned [6]. The changing variables, mT and hT, were validated through expected results also described in literature, specifically in [7].

Apart from plotting the state variables for the activation and inactivation of the sodium and potassium gates, membrane voltage state variables *Vm* and *VmT* were graphed separately. Seen in **Appendix A, Figure 10-12** are the Membrane Voltage vs. Time plots of singular axonal transmission with a voltage shift of 20 mV from the mTBI. These plots show the consistency of *Vm*, which is the membrane voltage for a healthy axon, and then show the differences in *VmT*, the membrane voltage with the trauma conditions affected by *fT*. From the graphs, it is evident that a greater impact on sodium gates due to trauma results in a more irregular and reduced amplitude of the neuron's action potential.

In **Appendix C, Table 2**, the equilibrium values for n, m, and h are shown calculated from **Equation 27, Appendix B**. These equilibrium values are critical to the model as they allow the model to only spike when a current input is added, instead of showing irregularities due to instabilities at the starting position. Also shown in the table are the maximum values for n, and m, and the minimum value for h, which are important for comparison with the values under the concussion conditions, as the values in **Appendix C, Table 2** all represent axonal transmission in an ideal state. Also shown is the value 35.9065 mV for the maximum *Vm*, which is important to note when analyzing the maximum VmT values to determine if there are any changes in the spike of the action potentials when an mTBI occurs.

Shown in **Appendix C, Table 3**, is the resulting equilibrium values, maximum, and minimum state variable values under the voltage shift and affected sodium gate percentage from the mTBI. In this table, there is an apparent trend that for the equilibrium values, the lower the voltage shift, the mT (sodium activation level) equilibrium value is larger, and the hT (potassium activation level) equilibrium value is smaller. This relationship can be seen in **Appendix A, Figure 13**. An interesting trend apparent in the mT maximum and hT minimum values is the differences between the 50% affected sodium gates and the 10% affected sodium gates. When comparing the values in each voltage shift category, the mT maximum values are greater for the 50% sodium gate percentage compared to the 10% percentage in both the 10 mV shift and the 14 mV shift. The same can be examined in the for the hT minimum value for the 20 mV voltage shift. Another interesting trend is the difference in the values for the 90% affected sodium gate percentage compared to the 10% and 50% values. While the 10% and 50% values are fairly similar for their mT maximum and hT minimum values in each voltage shift, the 90% has a large difference in values in comparison. It can also be examined that there is a larger difference in the values for the 50% affected sodium gates in the 20 mV shift, compared to the other shifts. The relationship being mT maximum values and hT minimum values can be seen in **Appendix A, Figure 14 and Figure 15** respectively.

When comparing the values produced for the maximum membrane voltage when impacted by different conditions involving concussion impacts, the results for the 10 mV voltage shift and the 14 mV voltage shift look fairly similar in the produced values depending on the sodium gate percentage. These values are both slightly less than the maximum membrane voltage for the perfect condition axonal transmission seen in **Appendix C, Table 3**. An interesting result for the 14 mV voltage shift is that the maximum VmT is slightly greater for 50% of affected sodium gates, compared to the 10%. The values examined for the 20 mV voltage shift are more linear for the resulting maximum VmT for each change in sodium gate percentage. The VmT value for the 10% affect sodium gates is significantly less than the maximum Vm for the perfect condition axonal transmission seen in **Appendix C, Table 3**, and the values examined for the 50% and 90% affected sodium gate percentage are more spread out than what can be examined for the 10 mV and 14 mV shift. The final trend to be examined from the data in **Appendix C, Table 3** is the consistency in maximum VmT values for the 90% affected sodium gates, with all of the values being around -48 mV no matter the voltage shift, indicating that in cases where large amount of sodium gates are impacted from a concussion, the acceleration of the high-speed impact is not relevant to the maximum membrane voltage produced from the action potential. The relationship for the maximum VmT values at the different affected sodium gate percentages, and different voltage shifts, can be seen in **Appendix A, Figure 16**. Putting everything together, **Appendix A, Figure 17** shows the correlation with the membrane voltages, conditional state variables, and current input in a singular axonal transmission.

Furthermore, the results from the optimization show convergence of the mean squared error over 700 epochs, as seen in **Appendix A, Figure 18.** The resultant coefficients are shown in **Appendix C, Table 4,** with the fT having a significantly higher magnitude coefficient, both fT and V_S being negative.

In addition to the voltage-shift damage model, an axon propagation synaptic transmission simulation was created, in order to model a damaged neuron network in comparison to a healthy one. Multiple spikes were simulated along the body of one neuron axon, depicting a simplified neuron model where action potentials are occurring across 8 nodes of ranvier [13], as can be seen in **Appendix A, Figure 19**. Maximum spike in a healthy neuron was 34.82 mV, and 21.45 mV in a traumatic neuron, under constant conditions of 40% sodium deactivation, and voltage shift of 20 mV. This was important for information transfer rate studies, as the voltage shifts and sodium gate activation translated to an increased active neuron time in damaged neurons of ~1.46 ms, depicted in **Appendix A, Figure 20**. The synaptic transmission as described in methods, used the voltage in a healthy neuron (Vm) and in a trauma induced neuron and (VmT) at a voltage shift of 20 mV, and sodium gate activation (fT) of 40%, to understand the effects on models across synapses of damage caused by concussion. The modified synaptic transmission spike can be seen in **Appendix A, Figure 21**, with the resulting multiple neuron propagation simulation and timing charts in **Appendix A, Figure 22 and 23.** The found voltage spikes with 36.55 mV and 15.83 mV, with a similar delay for a healthy synaptic, and traumatic synaptic neuron, respectively. Final simulation times for 4 neurons strung together with synaptic transmission current equations, resulted in 504.88 ms and 510.71 ms for healthy and damaged neurons, respectively - indicating this transmission model could scale to demonstrate the effects of concussion impact at the scale of a network of biologically spiking neurons and cognitive delay of deficit following TBIs.

Discussion

From the results of this investigation, it is evident that electrical activity of the neurons is negatively impacted as a result of concussions. Furthermore, it is emphasized that the degree of severity of the concussion as controlled by changing the initial velocity of the deceleration period and the percentage of damaged neurons, directly affect the severity of injury in the brain. The increase of velocity of the trauma causes a decrease in speed of both the activation state variable, and inactivation state variable of damaged sodium channels, and subsequently the action potential voltage. However, the more significant factor that decreases the magnitude and regularity of the voltage spike of the action potential is the percentage of active sodium channels, which at lower levels of voltage shifts, impact the maximum values of the activation and invasion state variables at 50% activity.

As the velocity parameter is increased, a higher voltage shift Vs is observed, causing the inactivation and activation rate to decrease in amplitude according to relative damage. In a physical brain, this slower rate decreases the speed of the action potential, leading to a reduction of neural impulse transmission, and cognitive delays. This compared to the sodium and potassium gate contents for the non-injury neuron model which do not change with a change in the voltage, further demonstrating the effect of the head trauma on the neurological physiology. The second parameter varied in the model, the percentage of activated neurons, fT, also demonstrates a significant effect on the regularity and amplitude of the action potential spike. When the percentage of active sodium channels is decreased, fewer sodium channels are available to participate in action potential generation, leading to a reduction in the magnitude of depolarization and a decrease in action potential amplitude. Additionally, the altered kinetics due to the decrease in active channels, cause irregularities and delays in the action potential spike, explaining the abnormal shape of the injured neuron spikes.

Furthermore, when examining the relationship between the activation and inactivation equilibrium points of the sodium channels with the voltage shift, there exists a linear relationship between these variables which trends inversely to its spike direction. This means that the voltage shift acts as an inhibitor to the activation and deactivation of the sodium gates, decreasing the efficiency of the action potential kinetics. In examining the relationship between the maximum and minimum values of the sodium channel activation constants, as well as the voltage shift and percent active sodium channels, an interesting interaction is observed. For the lower voltage shift values (10 mV and 14 mV) the minimum and maximum values for sodium activation and inactivation remain fairly constant with minute fluctuation for 0-50% sodium channel activation. However, from 50-100% activation this maximum value sharply declines inverse to its spike direction. This means that for low voltage shifts, the maximum level of activation and inactivation of ion gates remains at normal functioning levels. However, for a 20 mV voltage shift, although a similar trend is followed for the maximum and minimum values, there are irregularities at the 50% sodium channel activation compared to those for the 10 mV and 14 mV shift. This demonstrated that above a 14 mV shift and its 50% sodium gate activation, there is too severe of an impact for the gate constants to achieve their required maximum or minimum value. Thus, with this parameter in mind, the worst concussion symptoms before the gate constant amplitudes are impacted is 14 mV at 50% channel activity.

In interpreting the results from the optimization activity, one can clearly see the negative relationship between the voltage shift and percent of activated channels with the maximum voltage of the action potential. Interpreted from the negative sign of both coefficients, as the severity of these conditions increase, the action potential spike, and thus the impact on the brain increases. Notably, it emphasizes the significance of the percentage of active sodium channels over the voltage shift concerning the action potential spike. While both factors bear importance, the percentage of active sodium channels emerges as a superior predictor for potential axonal damage based on the magnitude of the coefficients. Hence, it is important to consider this factor in the overall model of the relationship between the velocity of impact and the final action potential spike.

Due to the time constraints of the project and a lack of testing around concussion pathology, aspects of the neuron model required simplification and abstraction to focus on specific behaviours of the neuron. Firstly, as touched on above, a recommendation for future work is to conduct experimental investigations into the correlation between concussion severity and the percentage of active neurons. By integrating these findings, the model can better predict the decline in action potential voltage, incorporating both factors of voltage shift and this percentage effectively. Future steps for the model would further add realism from a biological perspective, flushing out the layered neuron grouping projections connected using synaptic transmission. Neuron sizes could be varied in a network to have different sizes, node numbers, and diameter properties - which could be realized through implementation of cable theory for current conduction along the neuron bodies with varying dimensions. The transmission model should be incorporated for current from multiple neurons to feed the current into multiple other neurons. By building a network of neurons rather than focusing on a singular or linear path of neurons the interactions between the overall delay time of the synaptic transmission and the injection currents can be more biologically accurate. This will likely give more accurate results for total transmission times, allowing for a better understanding of cognitive delays in concussions.

As mentioned previously in the problem space, the clinical problem that this simulation intends on addressing is the lack of quantitative means in diagnosing concussions. Given the subjective nature of qualitatively assessing a patient based on their perceived cognitive impairment, there is a need for a more

defined method of determining concussion severity so that treatments can be personalized. It is noteworthy that virtually all concussions that occur result from unforeseen accidents [14]. With the exception of certain professional sports settings, this means that there are no accelerometers or other sensors that can map the components of the force transmitted during a concussion, leading to the inability to create a model with experimental data [14]. Although the devised model does not intend on addressing this clinical limitation, it does describe a methodology that can be applied to simulate the underlying neurodynamic processes that result, which could provide physicians with critical information necessary for rehabilitation procedures.

The results from the simulation give insight into several physiological processes such as the manner in which damage to voltage-gated sodium channels affects the transmission of an action potential, as well as the synaptic transmission of a signal. Specifically, the integration of the Hodgkin-Huxley model provides information about the threshold needed for an action potential to be initiated, as well as how the propagation is affected by the state of the sodium channels. Additionally, a modified HIC was introduced as a means of assessing concussion severity likelihood, which provides insight into how the concussions correspond to a voltage shift algorithm. This algorithm is what dictates the manner in which a more severe concussion leads to a greater decrease in transmission speeds and ultimately impairs cognitive function. One of the main limitations of this model is the use of three distinct concussion severities which corresponds to the three voltage shift values used. In future iterations, this could be expanded to a larger range to more accurately gauge the changes in action potential propagation that result from the damage to the sodium gates. Ideally, next steps would include the integration of the damage and network studies, so that velocity inputs could alter the voltages seen across action potentials in neurons in larger networks for full computational models that behave like biology under concussion scenarios.

References

[1] “Concussions: Symptoms, treatment and what you need to know,” UT Health San Antonio, https://www.uthscsa.edu/patient-care/physicians/news-item/concussions-symptoms-treatment-and-what-you-need-know#:~:text=As%20many%20as%203.8%20million,and%20what%20to%20look%20for (accessed Apr. 8, 2024).

[2] “TBI data,” Centers for Disease Control and Prevention, https://www.cdc.gov/TraumaticBrainInjury/data/index.html (accessed Apr. 8, 2024).

[3] C. C. Giza and D. A. Hovda, “The new neurometabolic cascade of concussion,” Neurosurgery, vol. 75, no. Supplement 4, Oct. 2014. doi:10.1227/neu.0000000000000505

[4] B. McHenery, “Head injury criterion and the ATB,” Head Injury Criterion and the ATB, https://mchenrysoftware.com/HIC and the ATB.pdf (accessed Mar. 15, 2024).

[5] H. Shi et al., “Demyelination as a rational therapeutic target for ischemic or traumatic brain injury,” Experimental Neurology, vol. 272, pp. 17–25, Oct. 2015. doi:10.1016/j.expneurol.2015.03.017

[6] M. Nelson and J. Rinzel, “ The Hodgkin-Huxley Model,” in *The Book of GENESIS*, New York, New York: GENESIS, 2003 (accessed Mar. 15, 2024).

[7] V. Volman and L. J. Ng, “Computer modeling of mild axonal injury: Implications for axonal signal transmission,” *Neural Computation*, vol. 25, no. 10, pp. 2646–2681, Oct. 2013. doi:10.1162/neco_a_00491

[8] W. Gerstner, “3.1 synapses,” 3.1 Synapses | Neuronal Dynamics online book, https://neuronaldynamics.epfl.ch/online/Ch3.S1.html#Ch3.E2 (accessed Mar. 15, 2024).

[9] M. Bourne, “Head injury criterion (HIC) pt 2: HIC index, example,” intmathcom RSS, https://www.intmath.com/applications-integration/hic-part2.php (accessed Apr. 8, 2024).

[10] J. A. Wang et al., “Membrane trauma and na+leak from nav1.6 channels,” American Journal of Physiology-Cell Physiology, vol. 297, no. 4, Oct. 2009. doi:10.1152/ajpcell.00505.2008

[11] *Synaptic transmission in the Central Nervous System (section 1, Chapter 6) neuroscience online: An electronic textbook for the Neurosciences: Department of Neurobiology and Anatomy - the University of Texas Medical School at Houston*. Synaptic Transmission in the Central Nervous System (Section 1, Chapter 6) Neuroscience Online: An Electronic Textbook for the Neurosciences | Department of Neurobiology and Anatomy - The University of Texas Medical School at Houston. (n.d.). https://nba.uth.tmc.edu/neuroscience/m/s1/chapter06.html#:~:text=For%20chemical%20synapses%2C%20there%20is,change%20in%20the%20postsynaptic%20cell

[12] W. J. Heitler, “The Hodgkin-Huxley Model for the Generation of Action Potentials,” The Hodgkin-Huxley model, https://www.st-andrews.ac.uk/~wjh/hh_model_intro/ (accessed Apr. 8, 2024).

[13] Z. M. Khaliq and I. M. Raman, “Axonal propagation of simple and complex spikes in cerebellar Purkinje neurons,” *The Journal of Neuroscience*, vol. 25, no. 2, pp. 454–463, Jan. 2005. doi:10.1523/jneurosci.3045-04.2005

[14] C. D. Gómez-Carmona, A. Bastida-Castillo, S. J. Ibáñez, and J. Pino-Ortega, “Accelerometry as a method for external workload monitoring in invasion team sports. A systematic review,” *PLOS ONE*, vol. 15, no. 8, Aug. 2020. doi:10.1371/journal.pone.0236643

Appendix A - Figures

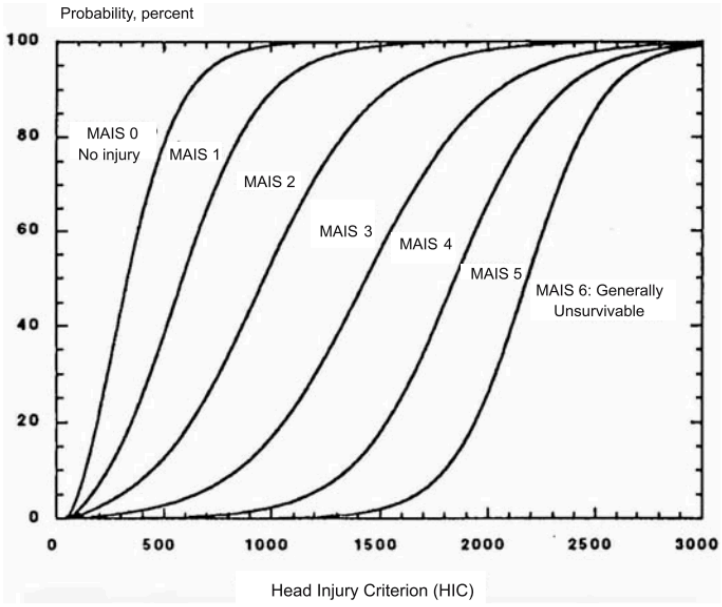

Figure 1. Probability of head injuries at different severities for given HIC values [4]

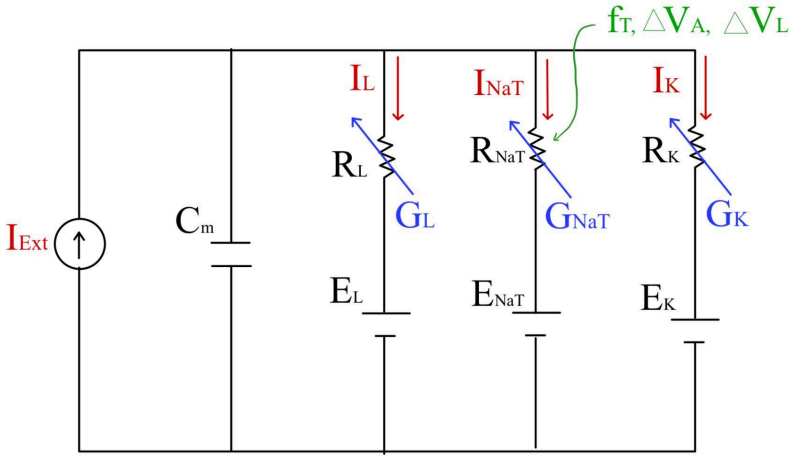

Figure 2. Hodgkin-Huxley Circuit Model adapted to incorporate NaV trauma.

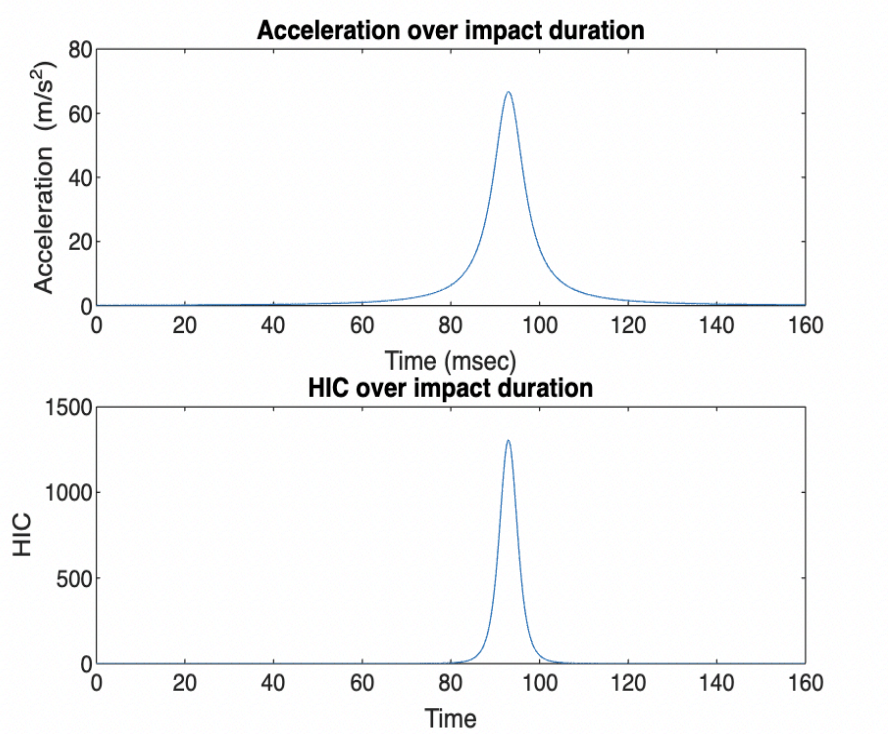

Figure 3. Acceleration and HIC over impact duration for 10 m/s velocity.

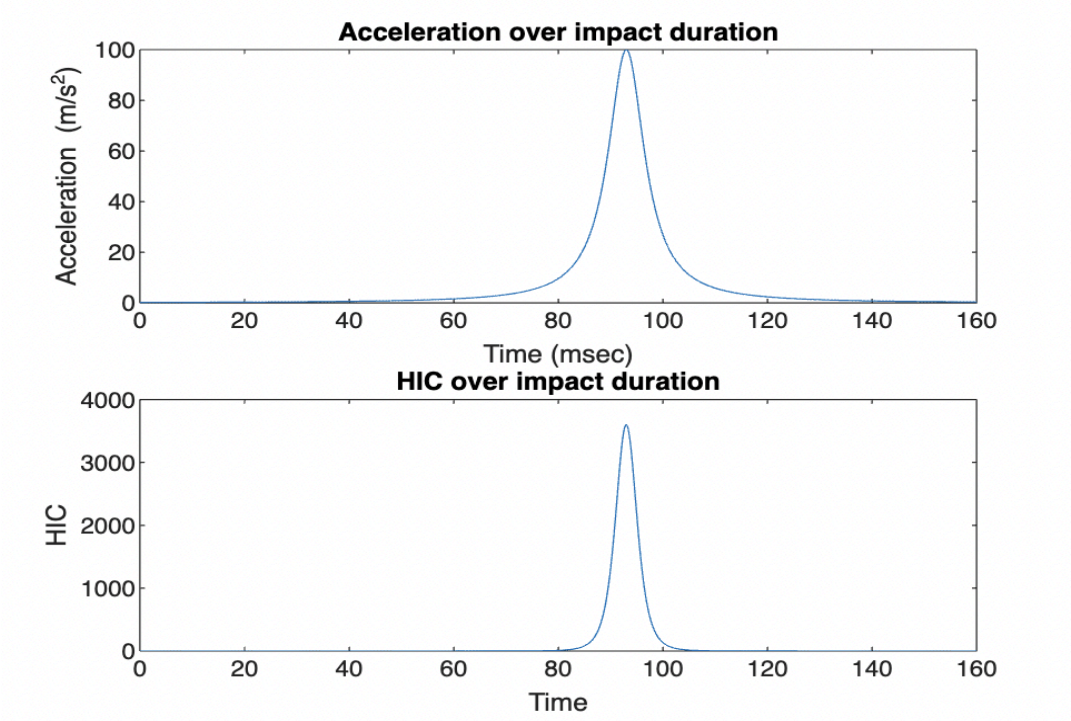

Figure 4. Acceleration and HIC over impact duration for 12 m/s velocity.

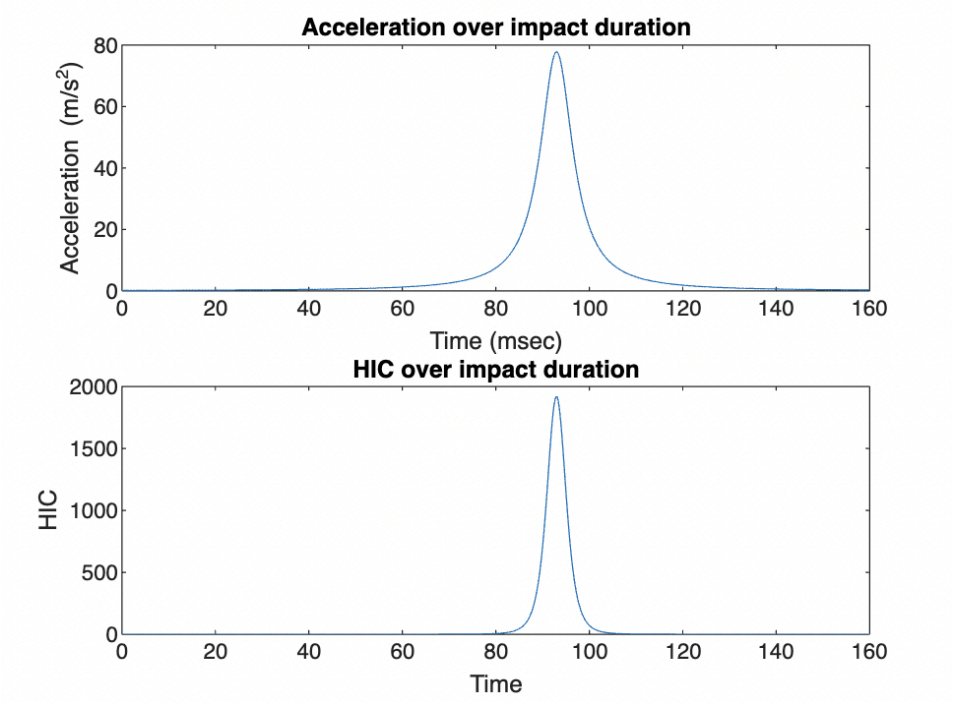

Figure 5. Acceleration and HIC over impact duration for 14 m/s velocity.

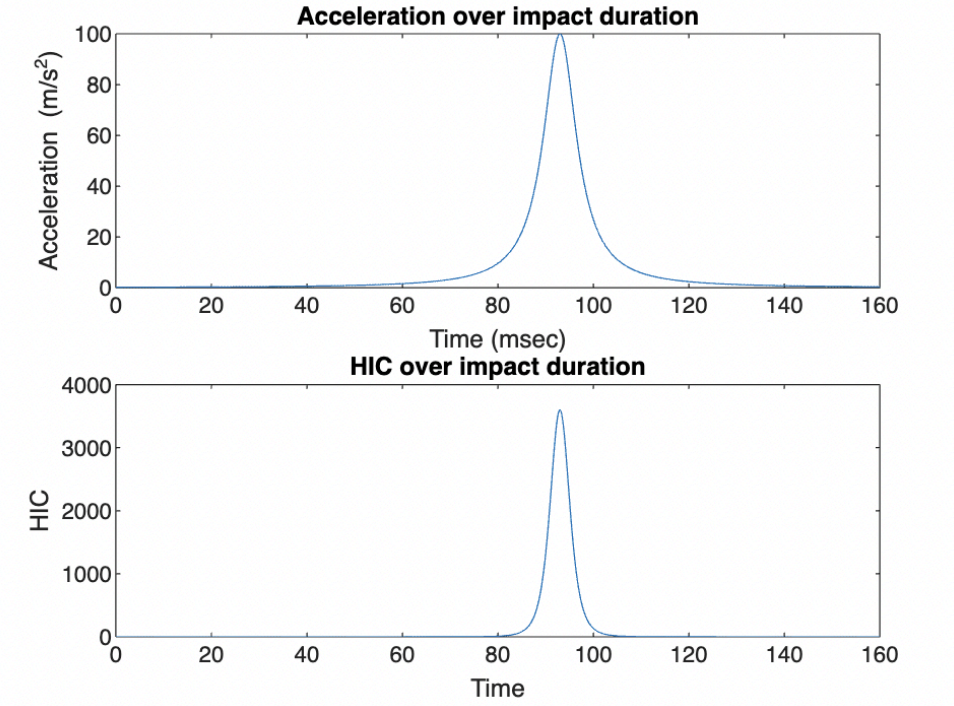

Figure 6. Acceleration and HIC over impact duration for 18 m/s velocity.

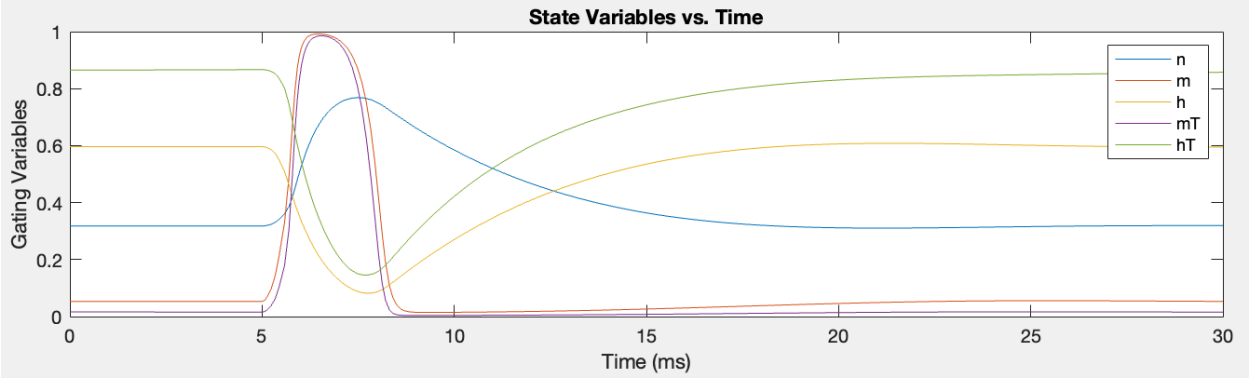

Figure 7. State variables with mild concussion levels (10 mV shift) with 10% of the sodium ion gates affected by the force impact.

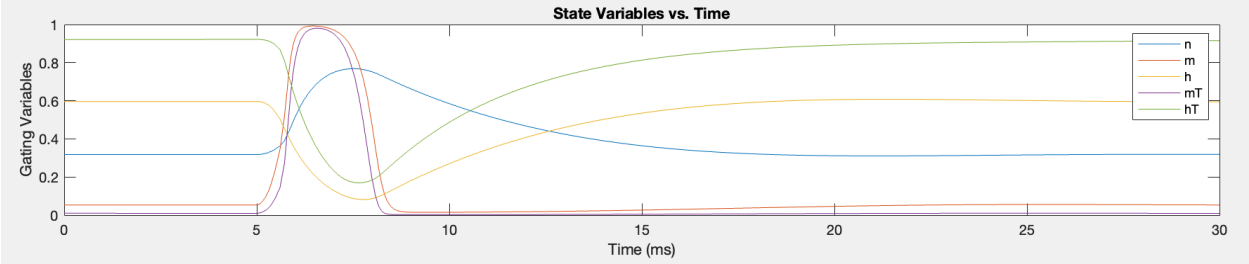

Figure 8. State variables with moderate concussion levels (14 mV shift) with 10% of the sodium ion gates affected by the force impact.

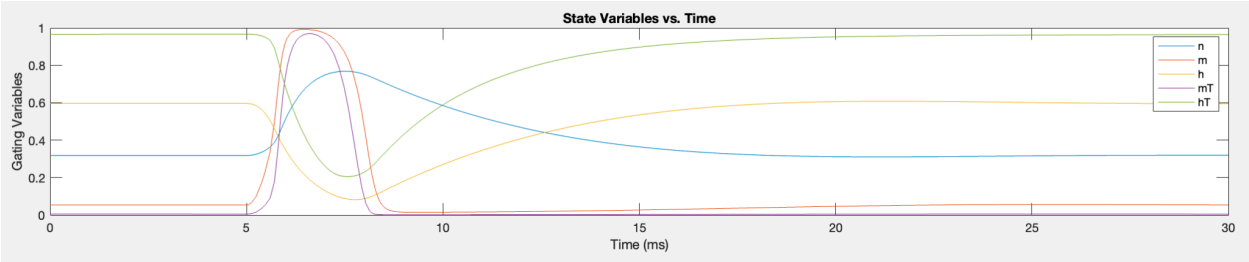

Figure 9. State variables with severe concussion levels (20 mV shift) with 10% of the sodium ion gates affected by the force impact.

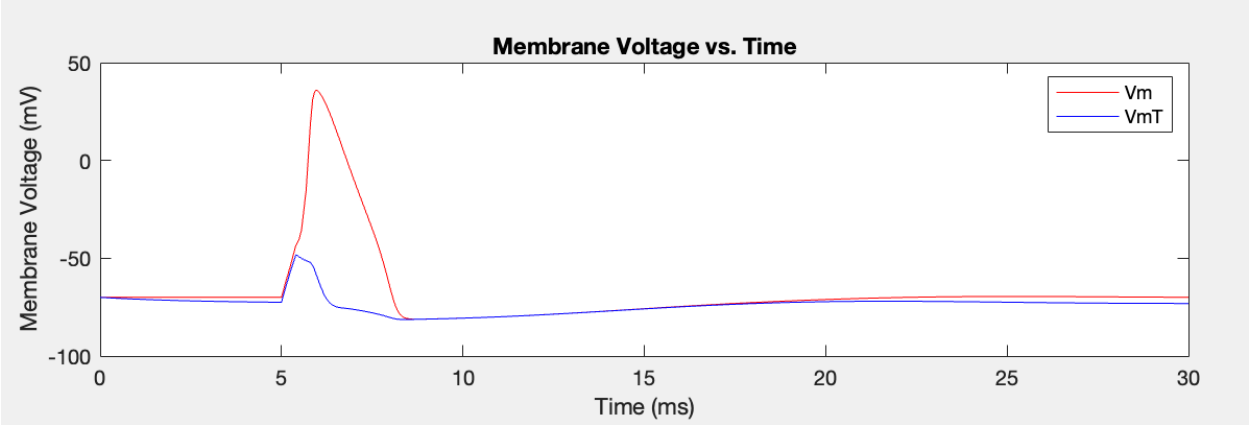

Figure 10. Voltage shift of 20 mV with 90% of the sodium ion gates affected by the force impact.

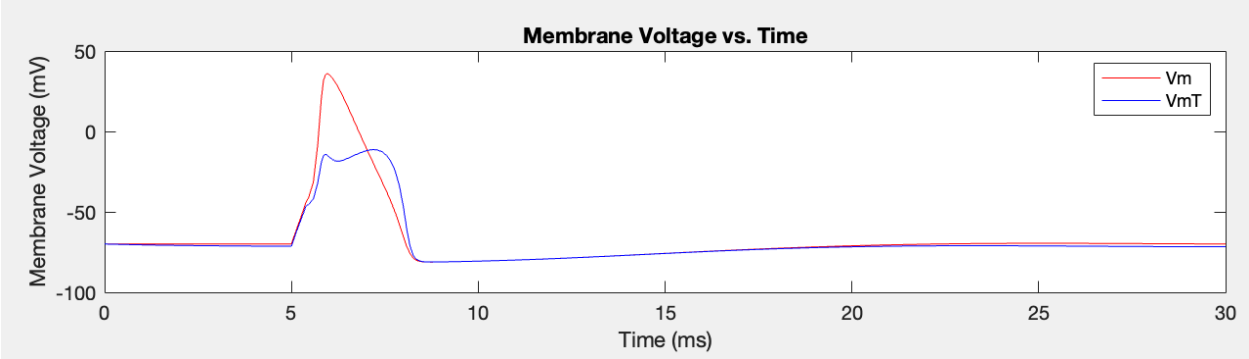

Figure 11. Voltage shift of 20 mV with 50% of the sodium ion gates affected by the force impact.

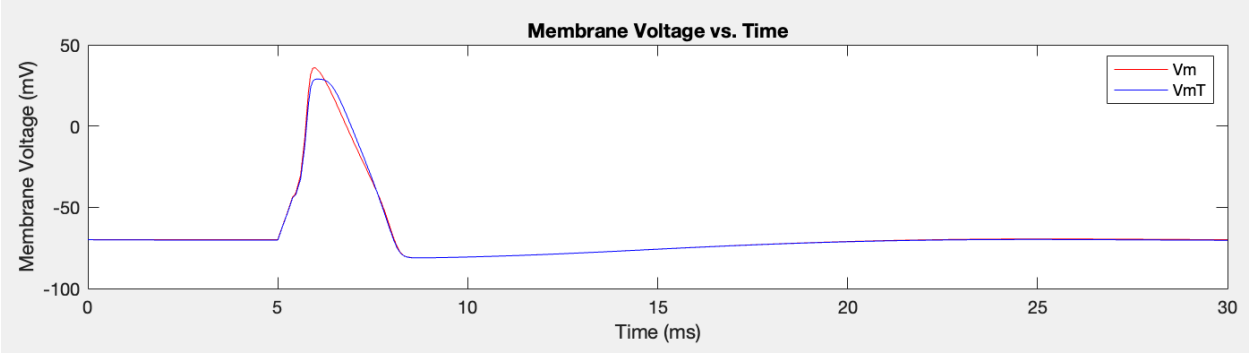

Figure 12. Voltage shift of 20 mV with 10% of the sodium ion gates affected by the force impact.

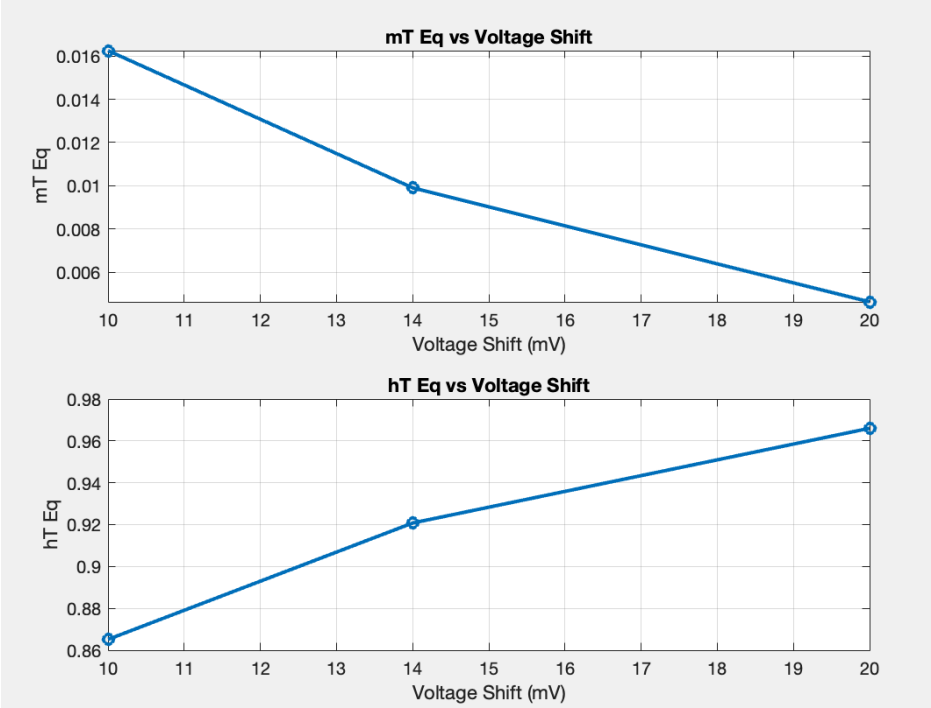

Figure 13. Comparison of mT equilibrium values and hT equilibrium values at voltage shifts of 10 mV, 14 mV, and 20 mV.

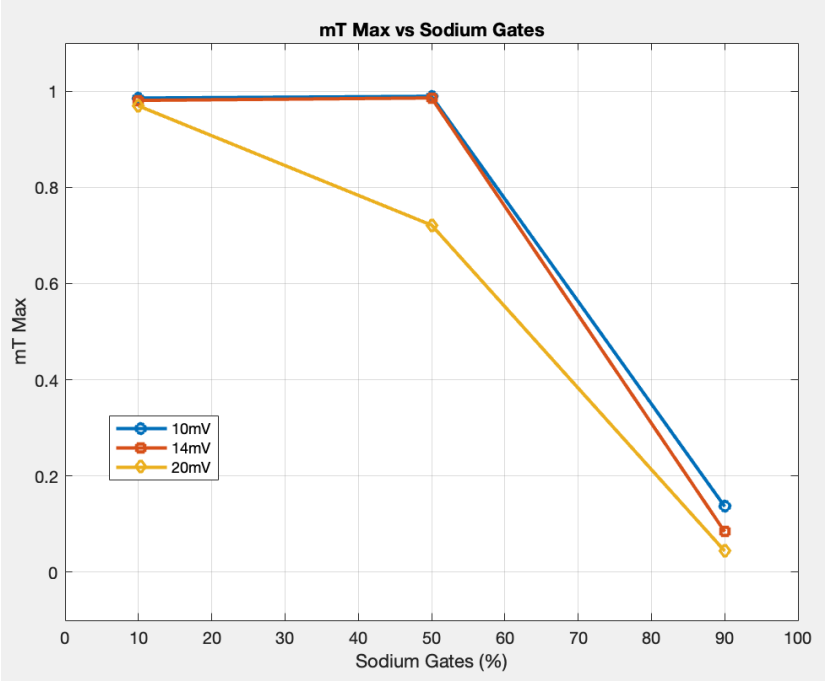

Figure 14. Comparison of mT maximums for 10%, 50%, and 90% affected sodium gates due to trauma, at voltage shifts 10 mV, 14 mV, and 20 mV.

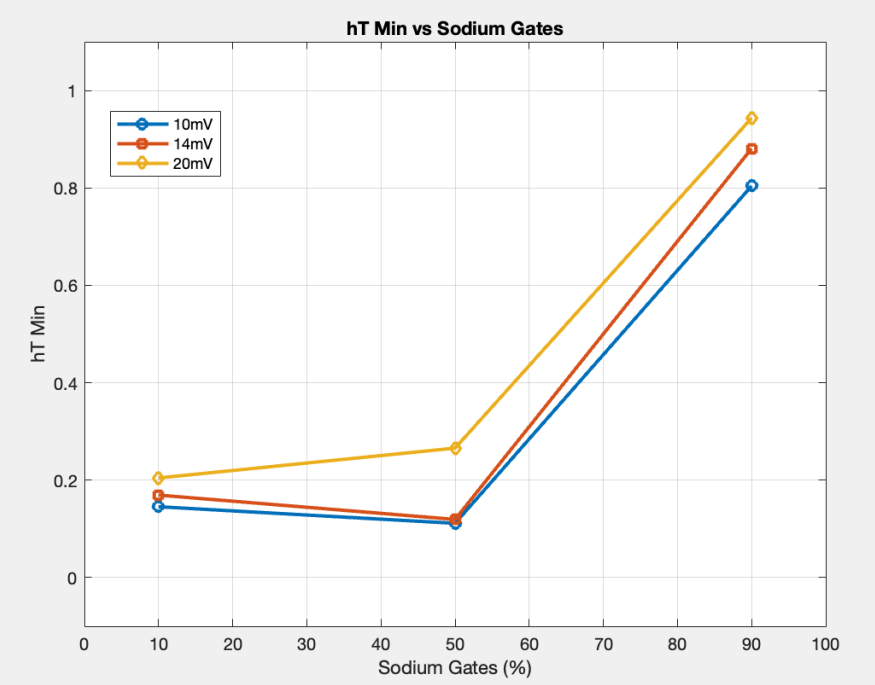

Figure 15. Comparison of hT minimums for 10%, 50%, and 90% affected sodium gates due to trauma, at voltage shifts 10 mV, 14 mV, and 20 mV.

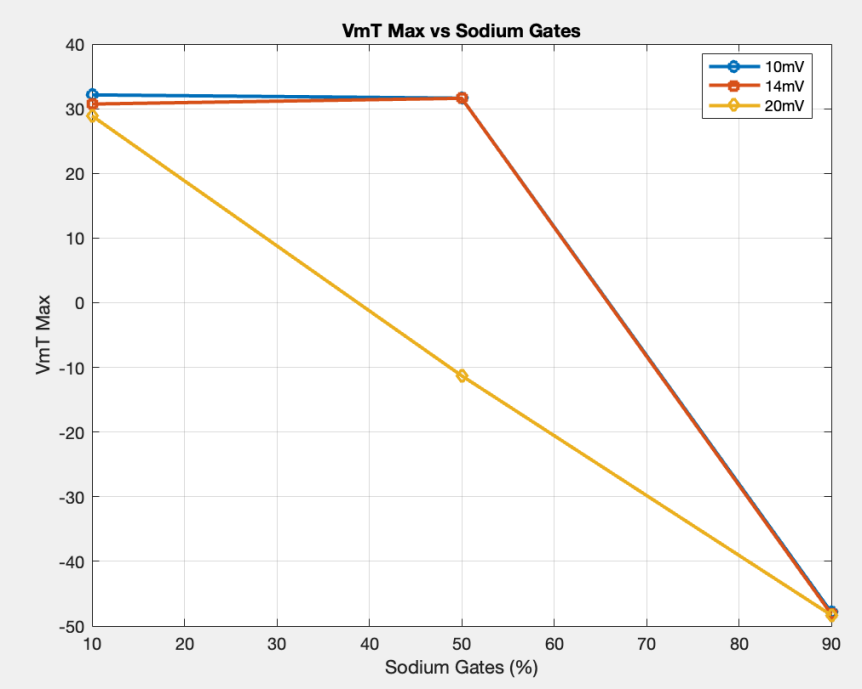

Figure 16. Comparison of membrane voltage maximums for 10%, 50%, and 90% affected sodium gates due to trauma, at voltage shifts 10 mV, 14 mV, and 20 mV.

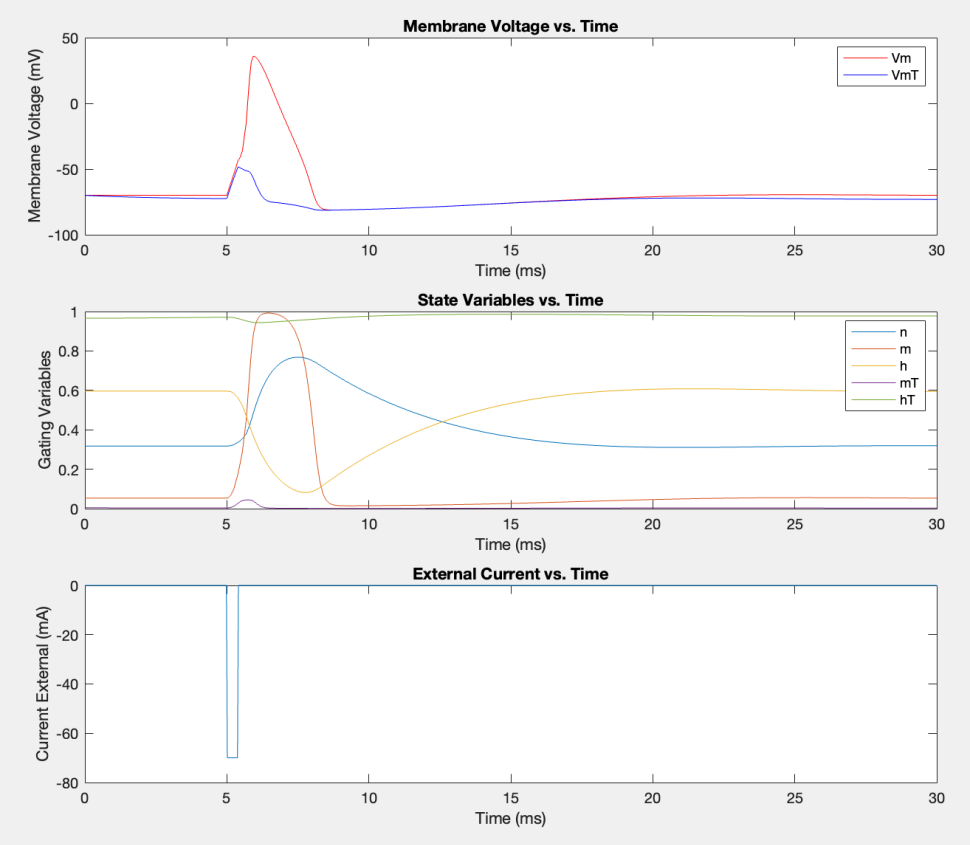

Figure 17. Comparison graph with current spike included for worst possible concussion conditions, involving a 20 mV voltage shift and 90% affected sodium gates for a singular neuron.

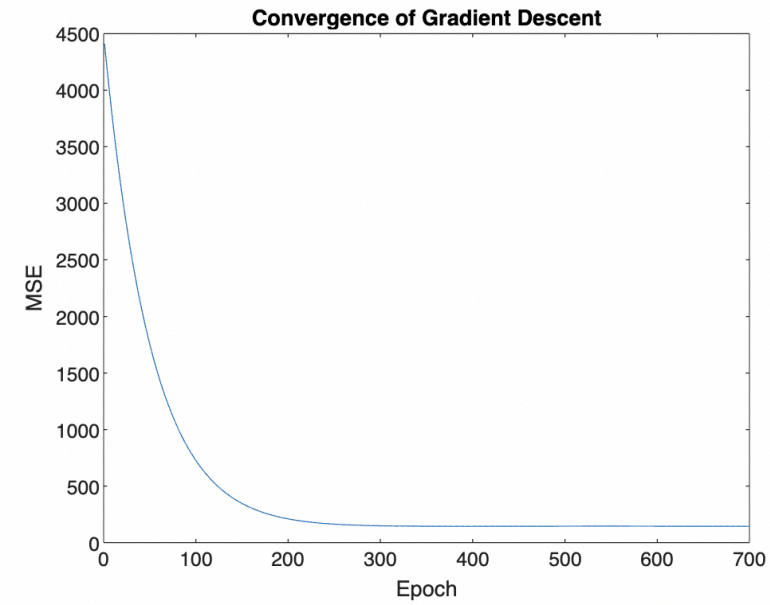

Figure 18. Mean Squared Error (MSE) across epochs

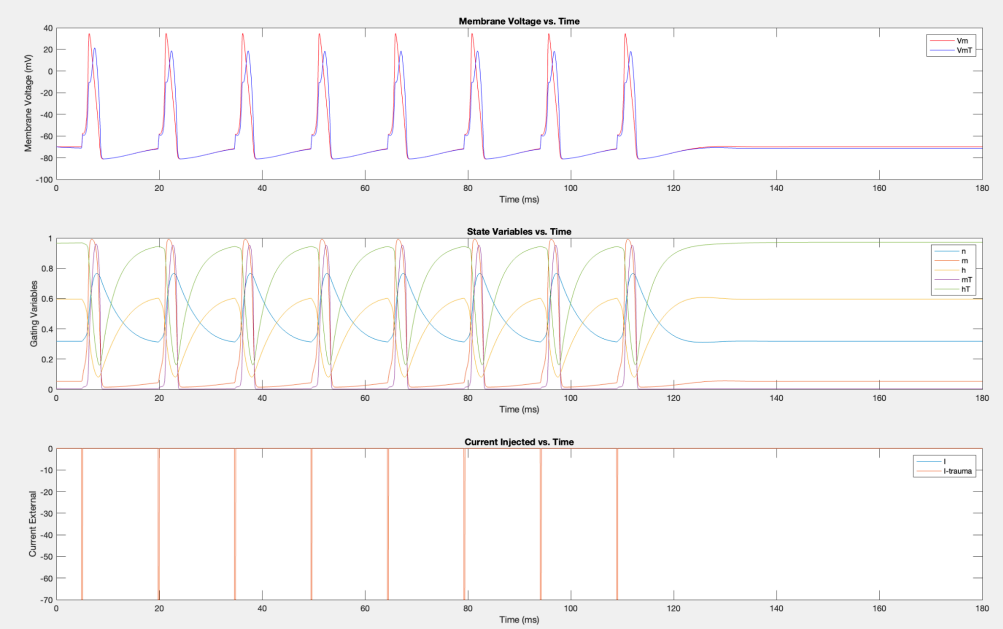

Figure 19. First modeled neuron, with multiple spike propagation (Trauma: fT = 40%, Vs = 20 mV)

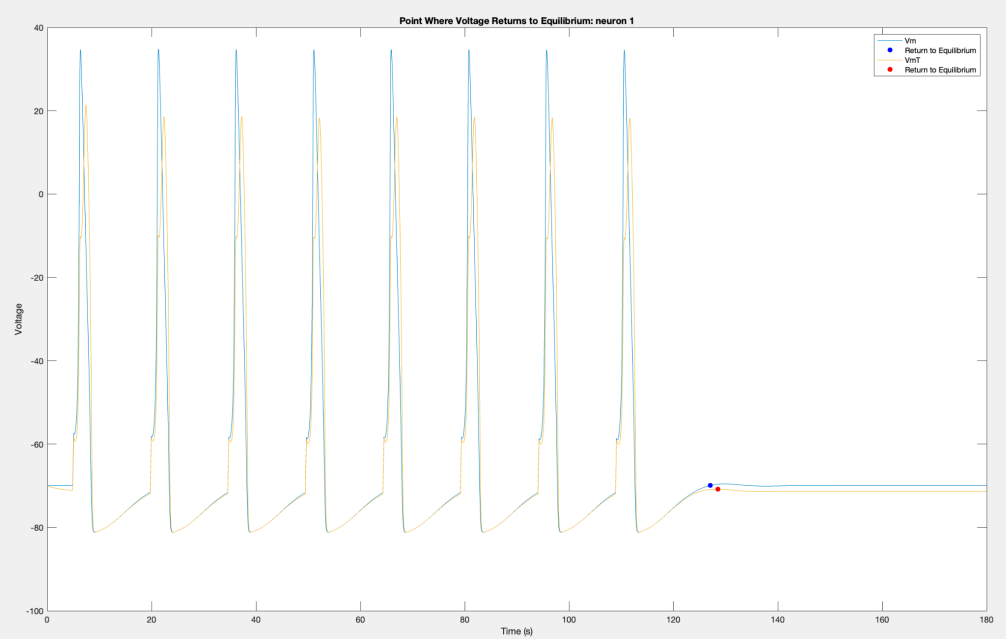

Figure 20. Multiple spike modeling timing across first neuron (excited externally) (Trauma: fT = 40%, Vs = 20 mV)

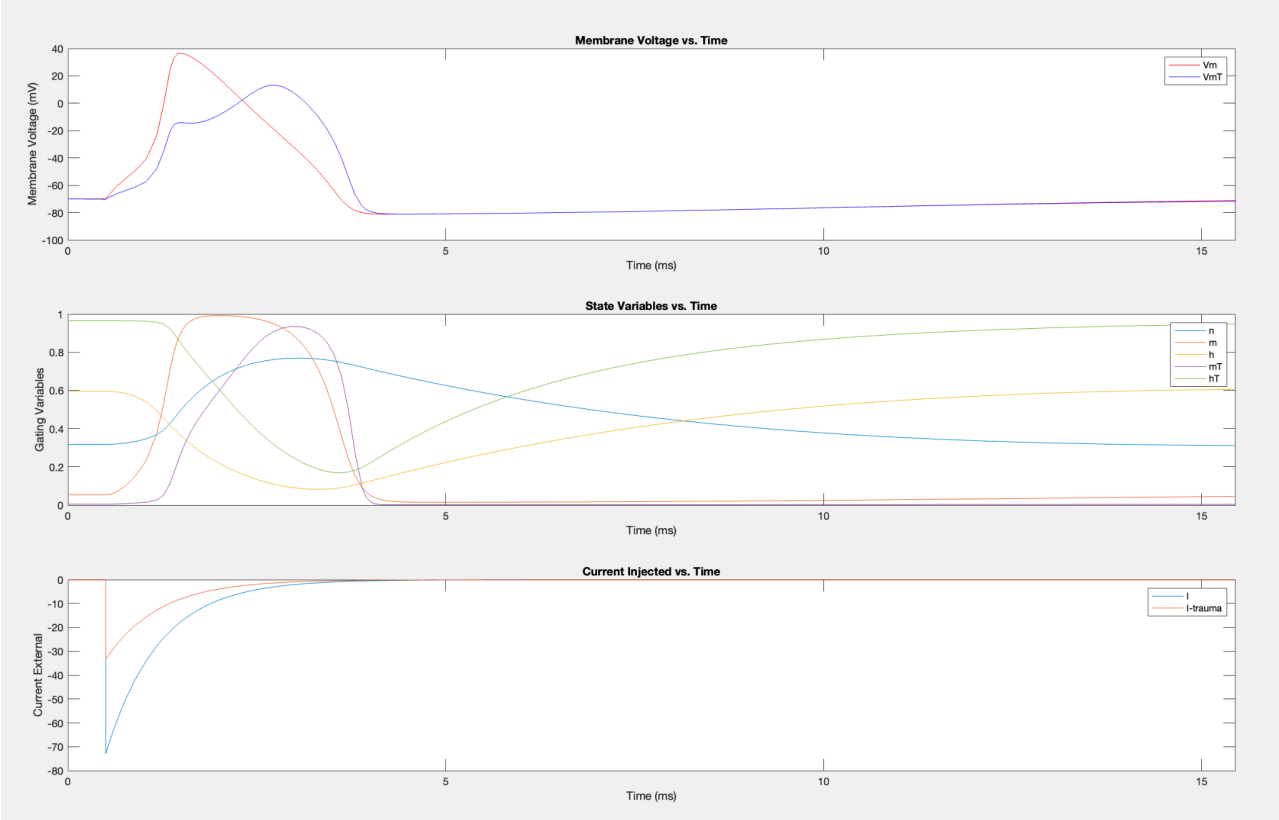

Figure 21. Single spike for synaptic transmission model (Trauma: fT = 40%, Vs = 20 mV)

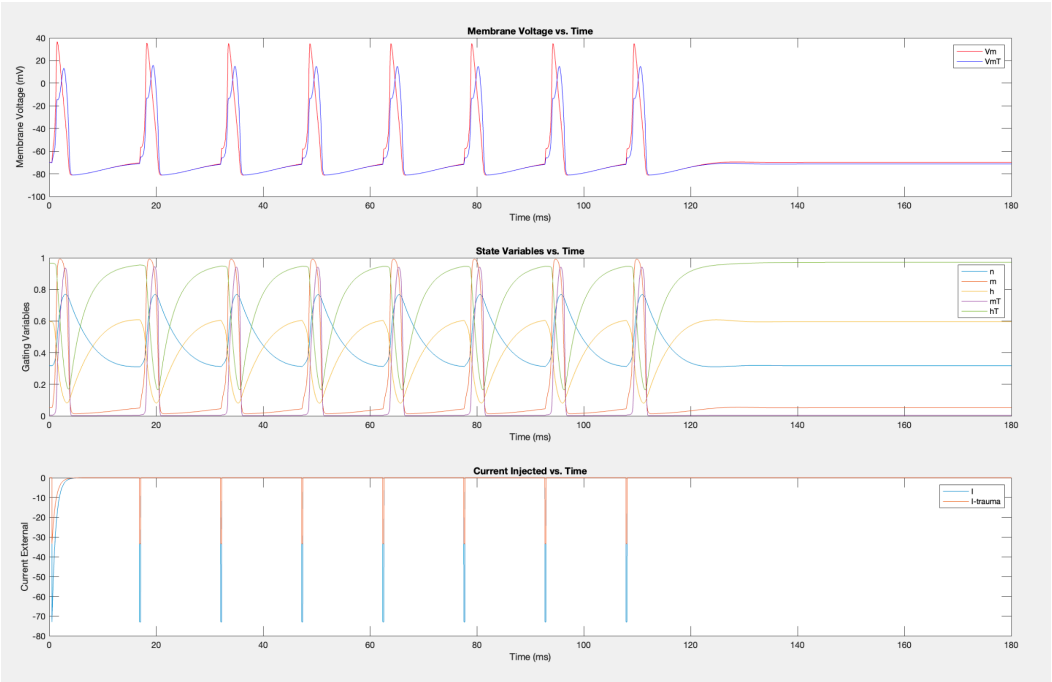

Figure 22. Synaptic transmission examination of a singular neuron with multiple spikes (Trauma: fT = 40%, Vs = 20 mV)

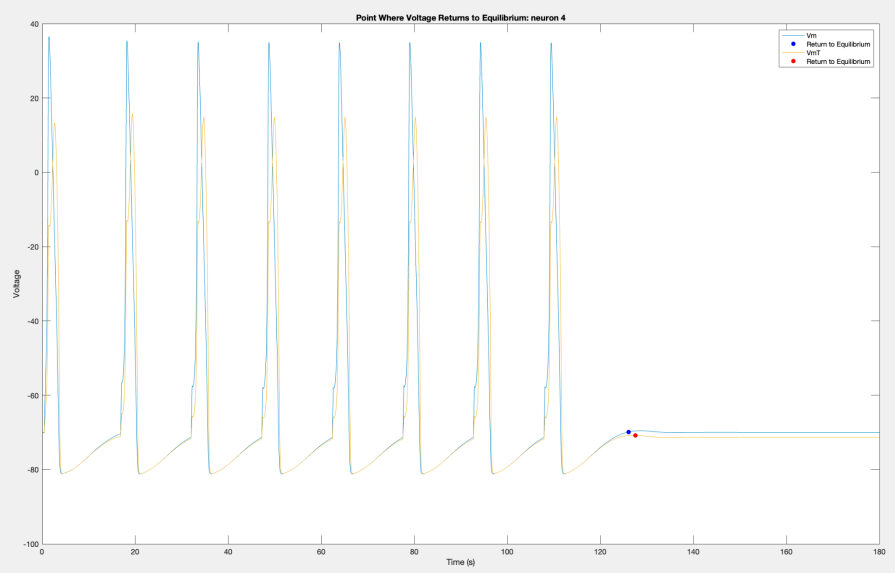

Figure 23. Multiple spike modeling timing across fourth synaptic neuron (Trauma: fT = 40%, Vs = 20 mV)

Appendix B - Equations

$$HIC = d\left[\frac{1}{d}\int_{t}^{t+d} a(T)dT\right]^{2.5} \quad \text{(Eq. 1)}$$

$$a(t) = \frac{16400}{(t-68)^2+400} + \frac{1480}{(t-93)^2+18} \quad \text{(Eq. 2)}$$

$$a(t) = \frac{v(t)}{(t-93)^2+18} \quad \text{(Eq. 3)}$$

$$I_{NaT} = g_{Na}[(1-f_T)m^3h + f_T m_T^3 h_T](V_m - E_{Na}) \quad \text{(Eq. 4)}$$

$$I_{Na} = g_{Na}m^3h(V_m - E_{Na}) \quad \text{(Eq. 5)}$$

$$I_K = g_k n^4(V_m - E_K) \quad \text{(Eq. 6)}$$

$$I_L = g_L(V_m - E_L) \quad \text{(Eq. 7)}$$

$$\frac{dm}{dt} = \alpha_m(1 - m) - \beta_m m \quad \text{(Eq. 8)}$$

$$\frac{dh}{dt} = \alpha_h(1 - h) - \beta_h h \quad \text{(Eq. 9)}$$

$$\frac{dn}{dt} = \alpha_n(1 - n) - \beta_n n \quad \text{(Eq. 10)}$$

$$\alpha_n = \frac{0.01(V_m+55)}{1-exp(-(V_m+55)/10)} \quad \text{(Eq. 11)}$$

$$\beta_n = 0.125exp(-(V_m + 65)/80) \quad \text{(Eq. 12)}$$

$$\alpha_m = \frac{0.1(V_m+25)}{1-exp(-(V_m+25)/10)} \quad \text{(Eq. 13)}$$

$$\beta_m = 4exp(\frac{V_m}{20}) \quad \text{(Eq. 14)}$$

$$\alpha_h = 0.07exp(\frac{V_m}{20}) \quad \text{(Eq. 15)}$$

$$\beta_h = \frac{1}{1+exp(-(V_m+30)/10)} \quad \text{(Eq. 16)}$$

$$\frac{dm_t}{dt} = \alpha_{mT}(1 - m_T) - \beta_{mT} m_T \quad \text{(Eq. 17)}$$

$$\frac{dh_T}{dt} = \alpha_{hT}(1 - h_T) - \beta_{hT} h_T \quad \text{(Eq. 18)}$$

$$\alpha_{mT} = \frac{0.1(V_{mT}+25+V_s)}{1-exp(-(V_{mT}+25+V_s)/10)} \quad \text{(Eq. 19)}$$

$$\beta_{mT} = 4exp((V_{mT} + V_s)/20) \quad \text{(Eq. 20)}$$

$$\alpha_{hT} = 0.07exp((V_{mT} + V_s)/20) \quad \text{(Eq. 21)}$$

$$\beta_{hT} = \frac{1}{1+exp(-(V_{mT}+30+V_s)/10)} \quad \text{(Eq. 22)}$$

$$\frac{dV_m}{dt} = -\frac{1}{C_m}[I_{ext} + \sum I_{Na} - \sum I_K - I_L] \quad \text{(Eq. 23)}$$

$$\frac{dV_{mT}}{dt} = -\frac{1}{C_m}[I_{ext} + \sum I_{NaT} - \sum I_K - I_L] \quad \text{(Eq. 24)}$$

$$I_{syn}(t) = g_{syn}(t)[V_m - E_{syn}] \quad \text{(Eq. 25)}$$

$$g_{syn}(t) = \sum_f \bar{g} exp[-(t - t^f)/\tau] \cdot H(t - t^f) \quad \text{(Eq. 26)}$$

$$P_x = \alpha_x / (\alpha_x + \beta_x) \quad \text{(Eq. 27)}$$

$$y = \beta_0 + \beta_1 x_1 + \beta_2 x_2 \quad \text{(Eq. 28)}$$

$$MSE = \frac{1}{N}\sum_{i=1}^{N}(y_i - (\beta_0 + \beta_1 x_{1i} + \beta_2 x_{2i})) \quad \text{(Eq. 29)}$$

$$\frac{\partial MSE}{\partial \beta_0} = \frac{-2}{N}\sum_{i=1}^{N}(y_i - (\beta_0 + \beta_1 x_{1i} + \beta_2 x_{2i})) \quad \text{(Eq. 30)}$$

$$\frac{\partial MSE}{\partial \beta_1} = \frac{-2}{N}\sum_{i=1}^{N} x_{1i}(y_i - (\beta_0 + \beta_1 x_{1i} + \beta_2 x_{2i})) \quad \text{(Eq. 31)}$$

$$\frac{\partial MSE}{\partial \beta_2} = \frac{-2}{N}\sum_{i=1}^{N} x_{2i}(y_i - (\beta_0 + \beta_1 x_{1i} + \beta_2 x_{2i})) \quad \text{(Eq. 32)}$$

Appendix C - Tables

Table 1. Hodgkin-Huxley constants

Constants	**Values**
g_{Na} (msiemens/cm^2)	120
g_L (msiemens/cm^2)	0.3
g_K (msiemens/cm^2)	36
E_{Na} (mV)	-115
E_L (mV)	-10.613
E_K (mV)	12
C_M (μF/cm^2)	1

Table 2. Consistent state variables for axonal transmission in a perfect condition

n Eq.	**m Eq.**	**h Eq.**	**n Max**	**m Max**	**h Min**	**Max Vm (mV)**
0.31768	0.052932	0.59612	~0.768	~0.992	~0.081	35.9065

Table 3. Consistent state variables for axonal transmission when impacted by an mTBI

Voltage Shift (mV)	**Sodium Gates (%)**	**mT Eq.**	**hT Eq.**	**mT Max**	**hT Min**	**Max VmT (mV)**
10	10	0.01625	0.86517	0.98558	0.14542	32.1356
	50			0.98916	0.11141	31.627
	90			0.13652	0.80405	-47.8846
14	10	0.009904	0.92078	0.98071	0.16933	30.7197
	50			0.98574	0.11936	31.6097
	90			0.08411	0.88095	-48.1503
20	10	0.004628	0.96602	0.96921	0.20451	28.899
	50			0.7214	0.26579	-11.2934
	90			0.044106	0.94355	-48.321

Table 4. Coefficients from optimization results

Coefficient	Value
β_0	-1.9236
β_1	-25.720
β_2	-77.1392